A 10-Vertex Iron−Dicarbollide System Formed by Insertion of {Fe(CO)$_4$} into 8-Vertex [*closo*-1-CB$_7$H$_8$]$^-$: Synthesis and Reactivity Studies

Andreas Franken, Thomas D. McGrath,* and F. Gordon A. Stone

Department of Chemistry & Biochemistry, Baylor University, Waco, Texas 76798-7348

Received August 29, 2007

Reaction of [NBu$^n_4$][*closo*-1-CB$_7$H$_8$] with [Fe$_2$(CO)$_9$] in refluxing THF (tetrahydrofuran) gives the neutral ferradicarborane [2,2,2-(CO)$_3$-1-OH-*closo*-2,1,10-FeC$_2$B$_7$H$_8$] (**3**), which, upon treatment with PEt$_3$ in the presence of Me$_3$NO, yields [2,2-(CO)$_2$-2-PEt$_3$-1-OH-*closo*-2,1,10-FeC$_2$B$_7$H$_8$] (**4**). In **3** and **4** the 10-vertex {FeC$_2$B$_7$} cluster has two carbon vertices in antipodal, four-connected positions and the iron atom in a five-coordinate site adjacent to a carbon vertex that bears an OH substituent. Treatment of **4** in THF with NaH and then R−X (X = Br, I) affords [2,2-(CO)$_2$-2-PEt$_3$-1-OR-*closo*-2,1,10-FeC$_2$B$_7$H$_8$] (R = Me (**5**), CH$_2$CH═CH$_2$ (**6**), CH$_2$C≡CH (**7**), CH$_2$C≡CMe (**8**)). The pendant allyl group in **6** becomes η^2-bonded to the iron center upon treatment with Me$_3$NO in CH$_2$Cl$_2$, giving [2-CO-2-PEt$_3$-1,2-σ:η^2-OCH$_2$CH═CH$_2$-*closo*-2,1,10-FeC$_2$B$_7$H$_8$] (**9**), which then with CNXyl (Xyl = C$_6$H$_3$Me$_2$-2,6) in the presence of PEt$_3$ gives [2,2-(CNXyl)$_2$-2-PEt$_3$-1-OCH$_2$CH═CH$_2$-*closo*-2,1,10-FeC$_2$B$_7$H$_8$] (**10**). Reaction between compound **7** and [Co$_2$(CO)$_8$] in petroleum ether yields [2,2-(CO)$_2$-2-PEt$_3$-1-{OCH$_2$-(μ-η^2:η^2-C≡CH)Co$_2$(CO)$_6$}-*closo*-2,1,10-FeC$_2$B$_7$H$_8$] (**12**), in which a {C$_2$Co$_2$} tetrahedron is linked to the 10-vertex {FeC$_2$B$_7$} cluster by an −OCH$_2$− bridge. Heating compound **7** with [Co(CO)$_2$(η-C$_5$H$_5$)] in refluxing toluene gives the complex [2,2-(CO)$_2$-2-PEt$_3$-1,4-μ-{OC(H)═C(Me)-*B*}-*closo*-2,1,10-FeC$_2$B$_7$H$_7$] (**13a**), which contains a 5-membered ring that involves one carbon vertex and an adjacent boron atom. Compound **13a** yields [2-CO-2,2-(PEt$_3$)$_2$-1,4-μ-{OC(H)═C(Me)-*B*}-*closo*-2,1,10-FeC$_2$B$_7$H$_7$] (**13b**) upon addition of further PEt$_3$ in the presence of Me$_3$NO. Treatment of compounds **7** and **8** with PEt$_3$ in CH$_2$Cl$_2$ and in the presence of Me$_3$NO affords the zwitterionic ylide species [2-CO-2-PEt$_3$-1,2-μ-{OCH$_2$C{═C(R′)PEt$_3$}}-*closo*-2,1,10-FeC$_2$B$_7$H$_8$] (R′ = H (**15**), Me (**17**), respectively). In the latter pair, an −OCH$_2$C{═C(R′)PEt$_3$} group bonded to a cage carbon atom is also directly σ-bonded (at the β-position) to the adjacent iron vertex, forming a 5-membered ring. The novel structural features of compounds **4**, **10**, **12**, **13**, **15**, and **17** have been confirmed by single-crystal X-ray diffraction studies.

Introduction

In metallacarborane chemistry there has traditionally been a disparity between the number of complexes of monocarbollide versus dicarbollide ligands, with the latter far outweighing the former.[1] The primary reason for this was the relatively limited availability of monocarbon carboranes compared to their dicarbon cousins,[2] as there were few simple and high-yielding routes to the monocarboranes from commercially available starting materials such as B$_{10}$H$_{14}$. In attempting to redress the monocarbollide/dicarbollide imbalance, we had been limited essentially to 12-vertex {MCB$_{10}$} species, as the {CB$_{10}$} carboranes were by far the most readily accessible.[3] Recently, however, there has been a resurgence in monocarborane chemistry, initiated by Brellochs,[4] which has led to straightforward procedures for the synthesis of monocarboranes with 7–10 vertices.[4,5] We have exploited the potential of this breakthrough to prepare a number of metal−monocarbollide species in the 9–11-vertex range,[6–13] several of which have displayed chemistry not seen in their larger cluster relatives. In one such system 9- and 10-vertex {FeCB$_7$} and {Fe$_2$CB$_7$} species were synthesized, but a trace third product defied

(1) Grimes, R. N. In *Comprehensive Organometallic Chemistry*; Wilkinson, G., Abel, E. W., Stone, F. G. A., Eds.; Pergamon Press: Oxford, U.K., 1982; Vol. 1, Section 5.5. Grimes, R. N. In *Comprehensive Organometallic Chemistry II*; Abel, E. W., Stone, F. G. A., Wilkinson, G., Eds.; Pergamon Press: Oxford, U.K., 1995; Vol. 1, Chapter 9.

(2) Stíbr, B. *Chem. Rev.* **1992**, *92*, 225.

(3) (a) McGrath, T. D.; Stone, F. G. A. *J. Organomet. Chem.* **2004**, *689*, 3891. (b) McGrath, T. D.; Stone, F. G. A. *Adv. Organomet. Chem.* **2005**, *53*, 1.

(4) Brellochs, B. In *Contemporary Boron Chemistry*; Davidson, M. G., Hughes, A. K., Marder, T. B., Wade, K., Eds.; Royal Society of Chemistry: Cambridge, U.K., 2000; p 212.

(5) (a) Stíbr, B.; Tok, O. L.; Milius, W.; Bakardjiev, M.; Holub, J.; Hnyk, D.; Wrackmeyer, B. *Angew. Chem., Int. Ed.* **2002**, *41*, 2126. (b) Franken, A.; Kilner, C. A.; Thornton-Pett, M.; Kennedy, J. D. *Collect. Czech. Chem. Commun.* **2002**, *67*, 869. (c) Jelínek, T.; Thornton-Pett, M.; Kennedy, J. D. *Collect. Czech. Chem. Commun.* **2002**, *67*, 1035. (d) Stíbr, B. *Pure Appl. Chem.* **2003**, *75*, 1295. (e) Brellochs, B.; Backovsky, J.; Stíbr, B.; Jelínek, T.; Holub, J.; Bakardjiev, M.; Hnyk, D.; Hofmann, M.; Císarová, I.; Wrackmeyer, B. *Eur. J. Inorg. Chem.* **2004**, 3605.

(6) Du, S.; Kautz, J. A.; McGrath, T. D.; Stone, F. G. A. *Organometallics* **2003**, *22*, 2842.

(7) (a) Du, S.; Farley, R. D.; Harvey, J. N.; Jeffery, J. C.; Kautz, J. A.; Maher, J. P.; McGrath, T. D.; Murphy, D. M.; Riis-Johannessen, T.; Stone, F. G. A. *Chem. Commun.* **2003**, 1846. (b) Du, S.; Jeffery, J. C.; Kautz, J. A.; Lu, X. L.; McGrath, T. D.; Miller, T. A.; Riis-Johannessen, T.; Stone, F. G. A. *Inorg. Chem.* **2005**, *44*, 2815.

(8) (a) Lei, P.; McGrath, T. D.; Stone, F. G. A. *Chem. Commun.* **2005**, 3706. (b) Lei, P.; McGrath, T. D.; Stone, F. G. A. *Organometallics* **2006**, *25*, 2011.

(9) Franken, A.; McGrath, T. D.; Stone, F. G. A. *Organometallics* **2005**, *24*, 5157.

(10) Franken, A.; McGrath, T. D.; Stone, F. G. A. *Inorg. Chem.* **2006**, *45*, 2669.

(11) Lu, X. L.; McGrath, T. D.; Stone, F. G. A. *Organometallics* **2006**, *25*, 2590.

10.1021/om700865s CCC: $40.75
Publication on Web 02/15/2008

Chart 1

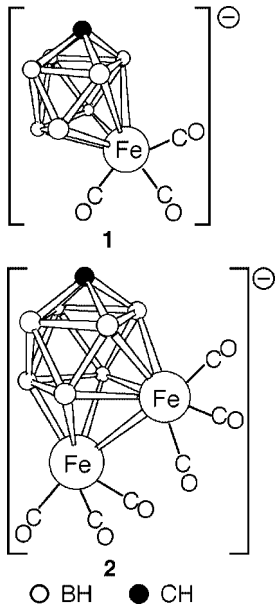

identification for some time. We now report upon the characterization and reactivity of this last species, ironically an iron−*di*carbollide cluster. Aspects of this work have already been communicated.[14]

Results and Discussion

Synthesis and Derivatization of C_{cage}−OH-Substituted {FeC_2B_7} Clusters. We have recently reported upon the reaction of $[NBu^n_4][closo\text{-}1\text{-}CB_7H_8]$ with $[Fe_3(CO)_{12}]$, in which $\{Fe(CO)_3\}$ fragments sequentially insert into the carborane to form the anionic mono- and diiron monocarbollide complexes $[7,7,7\text{-}(CO)_3\text{-}closo\text{-}7,1\text{-}FeCB_7H_8]^-$ (**1**) and then $[6,6,6,10,10,10\text{-}(CO)_6\text{-}closo\text{-}6,10,1\text{-}Fe_2CB_7H_8]^-$ (**2**), respectively (see Chart 1).[9] The same two anionic complexes are also formed when $[Fe(CO)_5]$ is used as the iron reagent, but yields are inferior and there is greater product contamination; use of $[Fe_2(CO)_9]$ gave only small quantities of **1** and **2**. However, such reactions involving this last, *diiron* carbonyl complex afforded a third ferracarborane species, compound **3**, in apparently good yields, as judged by ^{11}B NMR analysis of the reaction mixture. It was also observed that the same product was formed in the syntheses of **1** and **2** from the other iron carbonyls, but only in trace amounts (<5%).

Although the precise constitution of compound **3** eluded us for some time, it was ultimately identified as the 10-vertex iron−dicarbollide cluster $[2,2,2\text{-}(CO)_3\text{-}1\text{-}OH\text{-}closo\text{-}2,1,10\text{-}FeC_2B_7H_8]$ (see Chart 2) following an X-ray diffraction analysis upon crystals of a derivative (compound **4** below).[14] Chromatographic purification of **3** was difficult, as a consequence of the acidic cage-OH group, and this, combined with its contamination by higher nuclearity iron carbonyl hydride byproducts, seriously hindered its characterization. However, we found that addition of Me_3NO and PEt_3 resulted in substitution of one Fe-bound CO ligand in **3**, forming $[2,2\text{-}(CO)_2\text{-}2\text{-}PEt_3\text{-}1\text{-}OH\text{-}closo\text{-}2,1,10\text{-}FeC_2B_7H_8]$ (**4**). This treatment had the fortunate attendant benefit that it destroyed iron carbonyl hydride contaminants (apparently forming $[Fe_3(CO)_{12}]$); addition of small quantities of CF_3SO_3H to crude **3** similarly facilitated workup. In the case of **4**, the presence of the metal-bound phosphine donor reduced the acidity of the cage-OH moiety by destabilizing the conjugate base, allowing straightforward chromatographic purification. An X-ray diffraction experiment upon **4**[14] then confirmed the {*closo*-2,1,10-FeC_2B_7} architecture of this compound and hence of its parent **3**.

Chart 2

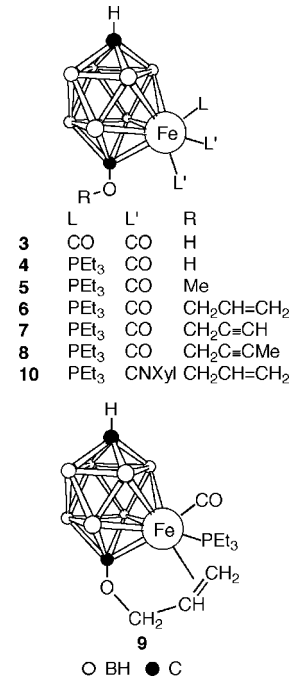

The structural study showed that both of the cluster carbon vertices are in antipodal, four-connected sites, as would be expected,[1,15] and the iron center is five-connected, also as anticipated. A most notable feature of the molecule is the terminal OH function that is bound to the carbon vertex adjacent to iron. This functional group is involved in hydrogen bonding to an adjacent molecule in the crystal, so that the two form weakly hydrogen bonded pairs as discussed previously.[14]

It is apparent that during formation of **3** a CO molecule has inserted into the carborane at the same time as the iron center, or else immediately before or after that event. The mechanism of such a reaction is not clear but it presumably involves an $\{Fe(CO)_4\}$ fragment: the yields of **3** being much higher from $[Fe_2(CO)_9]$ than from either $[Fe(CO)_5]$ or $[Fe_3(CO)_{12}]$ might suggest that the $\{Fe(CO)_4\}$ fragment forms more readily from the first reagent.[16] Initial interaction between the carborane and the iron moiety would be necessary to bring a metal-bound carbonyl into proximity with the cage, so that the CO ligand is activated toward cage insertion. At this point, for example, protonation of an {Fe−CO} unit would afford the carbyne {Fe≡COH}, which might readily penetrate the carborane to give the observed product; alternatively the hydroxyl oxygen might only become protonated by scavenging upon workup.

(12) (a) Du, S.; Kautz, J. A.; McGrath, T. D.; Stone, F. G. A. *Angew. Chem., Int. Ed.* **2003**, *42*, 5728. (b) McGrath, T. D.; Du, S.; Hodson, B. E.; Lu, X. L.; Stone, F. G. A. *Organometallics* **2006**, *25*, 4444. (c) McGrath, T. D.; Du, S.; Hodson, B. E.; Stone, F. G. A. *Organometallics* **2006**, *25*, 4452.

(13) Franken, A.; McGrath, T. D.; Stone, F. G. A. *J. Am. Chem. Soc.* **2006**, *128*, 16169.

(14) Franken, A.; Lei, P.; McGrath, T. D.; Stone, F. G. A. *Chem. Commun.* **2006**, 3423.

(15) (a) Williams, R. E. *Adv. Inorg. Chem. Radiochem.* **1976**, *18*, 67. (b) Ott, J. J.; Gimarc, B. M. *J. Am. Chem. Soc.* **1986**, *108*, 4303.

(16) Shriver, D. F.; Whitmire, K. H. In *Comprehensive Organometallic Chemistry*; Wilkinson, G., Abel, E. W., Stone, F. G. A., Eds.; Pergamon Press: Oxford, U.K., 1982; Vol. 4, Section 31.1.

Table 1. Analytical and Physical Data[a]

compd	ν_{max}(CO)[b]/cm^{-1}	anal./%[c] C	anal./%[c] H
[2,2,2-(CO)$_3$-1-OH-*closo*-2,1,10-$FeC_2B_7H_8$] (**3**)	2092 s, 2042 s	22.8 (22.7)	3.4 (3.4)
[2,2-(CO)$_2$-2-PEt$_3$-1-OH-*closo*-2,1,10-$FeC_2B_7H_8$] (**4**)	2019 s, 1971 s	33.8 (33.9)	6.6 (6.8)
[2,2-(CO)$_2$-2-PEt$_3$-1-OMe-*closo*-2,1,10-$FeC_2B_7H_8$] (**5**)	2015 s, 1967 s	36.0 (35.8)	7.3 (7.1)
[2,2-(CO)$_2$-2-PEt$_3$-1-OCH$_2$CH═CH$_2$-*closo*-2,1,10-$FeC_2B_7H_8$] (**6**)	2015 s, 1968 s	39.8 (39.5)	7.1 (7.2)
[2,2-(CO)$_2$-2-PEt$_3$-1-OCH$_2$C≡CH-*closo*-2,1,10-$FeC_2B_7H_8$] (**7**)	2018 s, 1970 s	40.0 (39.8)	6.6 (6.7)
[2,2-(CO)$_2$-2-PEt$_3$-1-OCH$_2$C≡CMe-*closo*-2,1,10-$FeC_2B_7H_8$] (**8**)	2017 s, 1969 s	41.1 (41.3)	6.7 (6.9)
[2-CO-2-PEt$_3$-1,2-σ:η^2-OCH$_2$CH═CH$_2$-*closo*-2,1,10-$FeC_2B_7H_8$] (**9**)	1964 s	39.4 (39.3)	7.5 (7.7)
[2,2-(CNXyl)$_2$-2-PEt$_3$-1-OCH$_2$CH═CH$_2$-*closo*-2,1,10-$FeC_2B_7H_8$] (**10**)		58.3 (57.9)	7.6 (7.7)
[2,2-(CO)$_2$-2-PEt$_3$-1-{OCH$_2$-(μ-η^2:η^2-C≡CH)Co_2(CO)$_6$}-*closo*-2,1,10-$FeC_2B_7H_8$] (**12**)	2095 m, 2056 m, 2027 s, 1969 s	33.7 (33.6)	3.7 (3.9)
[2,2-(CO)$_2$-2-PEt$_3$-1,4-μ-{OC(H)═C(Me)-*B*}-*closo*-2,1,10-$FeC_2B_7H_7$] (**13a**)	2018 s, 1970 s	39.5 (39.8)	6.9 (6.7)
[2-CO-2,2-(PEt$_3$)$_2$-1,4-μ-{OC(H)═C(Me)-*B*}-*closo*-2,1,10-$FeC_2B_7H_7$] (**13b**)	1926 s	44.6 (44.8)	8.5 (8.6)
[2-CO-2-PEt$_3$-1,2-μ-{OCH$_2$C{═C(H)PEt$_3$}}-*closo*-2,1,10-$FeC_2B_7H_8$] (**15**)	1906 s	44.9 (44.8)	8.6 (8.6)
[2-CO-2-PEt$_3$-1,2-μ-{OCH$_2$C{═C(Me)PEt$_3$}}-*closo*-2,1,10-$FeC_2B_7H_8$] (**17**)	1889 s	45.7 (45.9)	8.8 (8.7)

[a] All compounds are yellow, except compound **10**, which is orange, and compounds **12**, **15**, and **17**, which are red. [b] Measured in CH_2Cl_2; a broad, medium-intensity band observed at ca. 2500–2550 cm^{-1} in the spectra of all compounds is due to B−H absorptions. In addition, for compound **10**, ν_{max}(CN) 2088 s, 2043 s cm^{-1}. [c] Calculated values are given in parentheses. In addition, for compound **10**: % N, 4.7 (4.7).

Previous reports of carbon vertex incorporation via CO insertion into a boron cluster have been limited and include the reaction of Na[*nido*-$B_{10}H_{13}$] with [M(CO)$_6$] (M = Cr, Mo, W) under photochemical conditions[17]and the formation of iridacarboranes from a complex reaction between [IrCl(CO)(PPh$_3$)$_2$] and [*closo*-$B_{10}H_{10}$]$^{2-}$.[18] In our laboratories we have also recently shown that a carbonyl−molybdenum−monocarbollide trianion affords a molybdenum−dicarbollide cluster upon protonation in the presence of CO.[8b] However, the reaction forming compound **3** from [*closo*-1-CB_7H_8]$^-$ and iron carbonyls is unique in that it apparently has some generality with other transition-metal–carbonyl reagents: the corresponding {2,2,2-(CO)$_3$-1-OH-2,1,10-$MC_2B_7H_8$} species are also known for M = Ru, Mn, Re.[14]

The assumed structural similarity of compounds **3** and **4** is supported by the close similarity of much of their spectroscopic data (Tables 1−3). Both species show a 1:2:2:2 pattern of resonances in their $^{11}B\{^1H\}$ NMR spectra, consistent with the observed molecular C_s symmetry, but whereas the chemical shift range for **3** is δ +14.5 to −22.1, the range for **4** is +8.3 to −22.4. This may be a consequence of the increased electron density upon the metal following CO → PEt$_3$ substitution, but it can be dangerous to read too much into such shifts.[19] In their ^1H NMR spectra, broad signals are seen for the cage {CH} units at δ 6.16 (**3**) and 6.00 (**4**), typical for a four-connected {CH} vertex in 10-vertex clusters,[10,20] while the hydroxyl hydrogens resonate at δ 3.68 (**3**) and 3.69 (**4**) in the same spectra. Correspondingly, the two distinct types of cage carbon atom appear at very different positions in the $^{13}C\{^1H\}$ NMR spectra: the {CH} units give rise to broad signals at δ 80.4 (**3**) and 78.5 (**4**), whereas the {COH} groups resonate far downfield at δ 177.3 (**3**) and 184.5 (**4**).

The cage carbon bound hydroxyl group in both compounds **3** and **4** can readily be deprotonated by treatment with NaH in THF. In comparison to the spectra for their parents, the infrared spectra of the resulting anions showed a lowering in their CO stretching frequencies by tens of wavenumbers, as is to be expected upon anion formation. (For example, THF solutions of compound **4** turn darker yellow-orange upon deprotonation, with ν_{max}(CO) 1978 and 1927 cm^{-1}, and the $^{11}B\{^1H\}$ NMR chemical shift range also moves to lower frequency by 5–10 ppm: δ ca. +3 to −27.) Unfortunately, it was not possible to isolate and fully characterize these deprotonated species, as they were quite easily reprotonated by proton abstraction from solvents. However, in situ deprotonation followed by addition of a suitable organohalide reagent was a successful strategy for the introduction of other functional groups at the cage C−O terminus. Compound **4**, whose yield is superior and whose isolation and purification are much more straightforward, was the substrate of choice for these reactions.

Thus, reaction of **4** with NaH in THF followed by filtration to remove excess NaH and then addition of MeI afforded the cage-OMe species [2,2-(CO)$_2$-2-PEt$_3$-1-OMe-*closo*-2,1,10-$FeC_2B_7H_8$] (**5**). A similar protocol using various bromo reagents RBr gave the analogous compounds [2,2-(CO)$_2$-2-PEt$_3$-1-OR-*closo*-2,1,10-$FeC_2B_7H_8$] (R = CH$_2$CH═CH$_2$ (**6**), CH$_2$C≡CH (**7**), CH$_2$C≡CMe (**8**)), all in good yields. Data characterizing compounds **5**–**8** (see Chart 2) are given in Tables 1−3. All four species are straightforward derivatives of compound **4**, showing very similar NMR data for the {$FeC_2B_7H_8$} cage and the CO and PEt$_3$ ligands. In addition, signals are seen in the ^1H and $^{13}C\{^1H\}$ NMR spectra, corresponding to the various substituents attached via the cluster-bound oxygen. These occur in the expected positions and merit little further comment.

The presence of the strong donor PEt$_3$ bound to the iron center in compounds **4**–**8** results in a relatively high electron density at the metal center, evidenced by the rather low CO stretching frequencies (Table 1), so that substitution of a further CO ligand by donor groups such as PEt$_3$ and CNBu^t was neither expected nor observed, even in the presence of Me$_3$NO. On the other hand, it was hoped that the unsaturated organic moieties in

(17) Wegner, P. A.; Guggenberger, L. J.; Muetterties, E. L. *J. Am. Chem. Soc.* **1970**, *92*, 3473. See also: Schultz, R. V.; Sato, F.; Todd, L. J. *J. Organomet. Chem.* **1977**, *125*, 115. Fontaine, X. L. R.; Greenwood, N. N.; Kennedy, J. D.; MacKinnon, P. I.; Macpherson, I. *J. Chem. Soc., Dalton Trans.* **1987**, 2385.

(18) (a) Crook, J. E.; Greenwood, N. N.; Kennedy, J. D.; McDonald, W. S. *J. Chem. Soc., Chem. Commun.* **1981**, 933. (b) Crook, J. E.; Greenwood, N. N.; Kennedy, J. D.; McDonald, W. S. *J. Chem. Soc., Chem. Commun.* **1983**, 83.

(19) See, for example: Hermánek, S. *Chem. Rev.* **1992**, *92*, 325.

(20) See also, for example: (a) Stíbr, B.; Kennedy, J. D.; Thornton-Pett, M.; Dradáková, E. *Collect. Czech. Chem. Commun.* **1992**, *57*, 1439. (b) Evans, W. E.; Dunks, G. B.; Hawthorne, M. F. *J. Am. Chem. Soc.* **1973**, *95*, 4565. (c) Briguglio, J. J.; Sneddon, L. G. *Organometallics* **1986**, *5*, 327.

Table 2. ^{1}H and ^{13}C NMR Data[a]

compd	^{1}H/δ[b]	^{13}C/δ[c]
3	6.16 (br s, 1H, cage CH), 3.68 (br, 1H, OH)	204.3 (Fe−CO), 177.3 (br, cage COH), 80.4 (br, cage CH)
4	6.00 (br s, 1H, cage CH), 3.69 (br, 1H, OH), 1.94 (m, 8H, PCH_2), 1.22 (m, 12H, CH_3)	211.0 (d, J(PC) = 25, Fe−CO), 184.5 (br, cage COH), 78.5 (br, cage CH), 19.4 (d, J(PC) = 28, PCH_2), 7.4 (br, CH_3)
5	6.12 (br s, 1H, cage CH), 4.98 (s, 3H, OCH_3), 1.89 (m, 8H, PCH_2), 1.16 (m, 12H, CH_3)	211.1 (d, J(PC) = 24, Fe−CO), 189.7 (br, cage CO), 81.1 (br, cage C), 63.4 (OCH_3), 19.3 (d, J(PC) = 29, PCH_2), 7.3 (br, CH_3)
6	6.25 (m, 1H, =CH), 6.12 (br s, 1H, cage CH), 5.47 (dd, $J(HH)_{trans}$ = 18, $J(HH)_{gem}$ = 1, 1H, $=CH_2$), 5.30 (d, $J(HH)_{cis}$ = 10, 1H, $=CH_2$), 4.76 (d, J(HH) = 6, 2H, OCH_2), 1.91 (m, 6H, PCH_2), 1.18 (m, 9H, CH_3)	211.1 (d, J(PC) = 24, Fe−CO), 188.0 (br, cage CO), 134.6 (=CH), 117.4 ($=CH_2$), 81.0 (br, cage CH), 77.7 (OCH_2), 19.3 (d, J(PC) = 29, PCH_2), 7.6 (br, CH_3)
7	6.17 (br s, 1H, cage CH), 4.87 (s, 2H, OCH_2), 2.61 (s, 1H, ≡CH), 1.87 (m, 6H, PCH_2), 1.27 (m, 9H, CH_3)	210.8 (d, J(PC) = 24, Fe−CO), 185.7 (br, cage CO), 82.0 (br, cage CH), 79.5 (≡CH), 74.7 (≡*C*CH_2), 63.2 (OCH_2), 19.2 (d, J(PC) = 29, PCH_2), 7.5 (br, CH_3)
8	6.14 (br s, 1H, cage CH), 4.80 (s, 2H, OCH_2), 1.86 (m, 6H, PCH_2), 1.25 (s, 3H, ≡CCH_3), 1.17 (m, 9H, PCH_2CH_3)	210.9 (d, J(PC) = 25, Fe−CO), 186.5 (br, cage CO), 81.6 (br, cage CH), 64.1 (OCH_2), 74.9 (≡*C*CH_2), 83.0 (≡*C*CH_3), 19.3 (d, J(PC) = 29, PCH_2), 7.5 (br, PCH_2CH_3), 3.4 (≡*C*CH_3)
9	5.93 (br s, 1H, cage CH), 5.13 (d, $J(HH)_{trans}$ = 14, 1H, $=CH_2$) 4.89, 4.86 (m × 2, 1H × 2, OCH_2), 3.62 (d, $J(HH)_{cis}$ = 9, 1H, $=CH_2$), 2.64 (dd, 1H, =CH), 1.71 (m, 6H, PCH_2), 1.04 (m, 9H, CH_3)	219.5 (d, J(PC) = 36, Fe−CO), 198.2 (br, cage CO), 88.5 ($=CH_2$ or OCH_2), 77.0 ($=CH_2$ or OCH_2), 74.3 (br, cage CH), 54.2 (d, J(PC) = 6, =CH), 19.5 (d, J(PC) = 29, PCH_2), 8.7 (d, J(PC) = 5, CH_3)
10	7.05 (br m, 6H, C_6H_3), 6.26 (m, 1H, =CH), 5.94 (br s, 1H, cage CH), 5.39, 5.19 (d × 2, J(HH) = 10, 1H + 1H, $=CH_2$), 4.74 (m, 2H, OCH_2), 2.42 (s, 12H, $C_6H_3CH_3$), 1.90 (m, 6H, PCH_2), 1.13 (m, 9H, PCH_2CH_3)	182.0 (br, cage CO), 135.8 (=CH), 134.5–126.5 (C_6H_3), 130.2 (d, J(PC) = 11, C≡N), 115.9 ($=CH_2$), 79.5 (br, cage CH), 76.8 (OCH_2), 25.6 ($C_6H_3CH_3$), 18.9 (d, J(PC) = 27, PCH_2), 7.9 (br, PCH_2CH_3)
12	6.24 (s, 1H, Co_2C≡CH), 6.19 (br s, 1H, cage CH), 5.46 (s, 2H, OCH_2), 1.94 (m, 6H, PCH_2), 1.20 (m, 9H, CH_3)	210.9 (d, J(PC) = 24, Fe−CO), 199.6 (br, Co−CO), 187.0 (br, cage CO), 90.6 (Co_2C≡CH), 82.2 (br, cage CH), 77.0 (OCH_2), 73.2 (Co_2C≡*C*H), 19.4 (d, J(PC) = 29, PCH_2), 7.6 (br, CH_3)
13a	8.00 (s, 1H, =CH), 5.46 (br s, 1H, cage CH), 1.87 (m, 6H, PCH_2), 1.78 (s, 3H, =CCH_3), 1.20 (m, 9H, PCH_2CH_3)	211.4 (d, J(PC) = 23, Fe−CO), 183.9 (br, cage CO), 169.3 (=CH), 129.5 (vbr, =*C*CH_3), 65.8 (br, cage CH), 19.2 (d, J(PC) = 28, PCH_2), 12.0 (=*C*CH_3), 7.4 (br, PCH_2CH_3)
13b	8.02 (s, 1H, =CH), 5.41 (br s, 1H, cage CH), 1.86 (m, 12H, PCH_2), 1.81 (s, 3H, =CCH_3), 1.17 (m, 18H, PCH_2CH_3)	215.7 (t, J(PC) = 27, Fe−CO), 182.0 (br, cage CO), 167.4 (=CH), 127.9 (vbr, =*C*CH_3), 66.4 (br, cage CH), 20.1 (d, J(PC) = 25, PCH_2), 12.1 (=*C*CH_3), 8.4 (br, PCH_2CH_3)
15	ca. 5.8 (vbr, 1H, cage CH),[d] 5.62, 5.52 (m × 2, 1H × 2, OCH_2), 5.36 (ddt, ^{2}J(PH) = 29, ^{4}J(PH) = 4, ^{4}J(HH) = 2, =*CH*PEt_3), 2.02 (m, 6H, PCH_2), 1.79, 1.62 (m × 2, 3H × 2, PCH_2), 1.17 (m, 9H, CH_3), 0.98 (m, 9H, CH_3)	218.4 (d, J(PC) = 32, Fe−CO), 194.0 (br, cage CO), 91.3 (dd, J(PC) = 14 and 1, =CFe), 89.0 (d, J(PC) = 60, =$CPEt_3$), 72.4 (br, OCH_2), 51.8 (br, cage C), 17.8 (d, J(PC) = 26, PCH_2), 15.0 (d, J(PC) = 51, PCH_2), 7.9 (d, J(PC) = 5, CH_3), 5.9 (d, J(PC) = 5, CH_3)
17	ca. 5.9 (vbr, 1H, cage CH),[d] 5.64, 5.42 (m × 2, 1H × 2, OCH_2), 2.24 (d, J(PH) = 13, =CMe), 2.06 (m, 6H, PCH_2), 1.79, 1.61 (m × 2, 3H × 2, PCH_2), 1.16 (m, 9H, CH_3), 1.00 (m, 9H, CH_3)	217.0 (d, J(PC) = 32, Fe−CO), 193.2 (br, cage CO), 96.4 (d, J(PC) = 46, =$CPEt_3$), 91.1 (dd, J(PC) = 17 and 3, =CFe), 70.4 (br, cage C), 60.0 (br, OCH_2), 25.9 (dd, J(PC) = 21 and 2, =*C*CH_3), 18.6 (d, J(PC) = 24, PCH_2), 15.2 (d, J(PC) = 47, PCH_2), 8.5 (d, J(PC) = 6, PCH_2CH_3), 6.2 (d, J(PC) = 4, PCH_2CH_3)

[a] Chemical shifts (δ) are given in ppm and coupling constants (J) in hertz; measurements were carried out at ambient temperatures in CD_2Cl_2. [b] Resonances for terminal BH protons occur as broad unresolved signals in the range δ ca. −1 to +3. [c] ^{1}H-decoupled chemical shifts are positive to high frequency of $SiMe_4$. [d] Tentative assignment.

Table 3. ^{11}B and ^{31}P NMR Data[a]

compd	^{11}B/δ[b]	^{31}P/δ [c]
3	14.5, −0.3 (2B), −15.7 (2B), −22.1 (2B)	
4	8.3, −1.0 (2B), −17.4 (2B), −22.4 (2B)	54.8
5	7.1, −1.0 (2B), −19.5 (2B), −22.2 (2B)	54.7
6	7.0, −1.1 (2B), −19.2 (2B), −22.1 (2B)	54.5
7	6.3, −1.0 (2B), −18.9 (2B), −22.0 (2B)	54.7
8	7.1, −0.9 (2B), −19.0 (2B), −22.0 (2B)	54.7
9	1.5, −2.2, −8.2, −16.8, −20.2 (2B), −22.3	50.6
10	3.6, −0.6 (2B), −20.6 (2B), −23.1 (2B)	54.0
12	7.7, −0.9 (2B), −19.3 (2B), −22.0 (2B)	53.9
13a	14.4 (B(4)), 0.2 (2B), −17.0 (2B), −24.9 (2B)	54.8
13b	11.3 (B(4)), −0.1 (2B), −19.4 (2B), −25.3 (2B)	41.5
15	−3.8, −5.8, −10.8, −13.1, −20.4, −23.9, −26.3	50.9 ($FePEt_3$), 6.9 (=$CPEt_3$)
17	−2.6 (2B), −8.5, −13.1, −20.8, −24.2, −24.9	53.0 ($FePEt_3$), 15.5 (=$CPEt_3$)

[a] Chemical shifts (δ) are given in ppm and coupling constants (J) in Hz,; measurements were carried out at ambient temperatures in CD_2Cl_2. [b] ^{1}H-decoupled chemical shifts are positive to high frequency of $BF_3\cdot Et_2O$ (external); resonances are of unit integral except where indicated. [c] ^{1}H-decoupled chemical shifts are positive to high frequency of 85% H_3PO_4 (external).

compounds **6–8**, since they are attached to a cage vertex adjacent to the metal center, might be able to become π-bound to the iron through formation of an intramolecular five- or six-membered ring. Such a situation would be highly favorable, and it was anticipated that this could be sufficient to overcome the reluctance of the CO ligands toward substitution. Not surprisingly, rather different results were found for the double-bond compound versus the triple-bond systems, of which the former is discussed first.

Reactions of the C_{cage}−O−Allyl Derivative 6. Treatment of **6** with Me_3NO in CH_2Cl_2 afforded, as hoped, the compound [2-CO-2-PEt_3-1,2-σ:η^2-OCH_2CH=CH_2-*closo*-2,1,10-$FeC_2B_7H_8$] (**9**) (see Chart 2). Unfortunately, crystals suitable for an X-ray diffraction structural study upon **9** were not

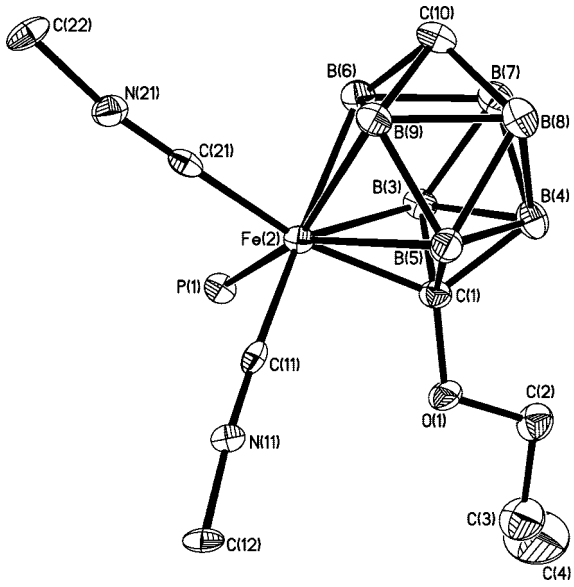

Figure 1. Structure of compound **10** showing the crystallographic labeling scheme. In this and subsequent figures, thermal ellipsoids are shown at the 40% probability level, phosphorus-bound ethyl groups are omitted, and only chemically important H atoms are shown. Selected distances (Å) and angles (deg): Fe(2)−C(1) = 1.961(3), Fe(2)−P(1) = 2.2219(10), Fe(2)−C(11) = 1.832(3), Fe(2)−C(21) = 1.821(4), C(1)−O(1) = 1.409(4), O(1)−C(2) = 1.439(4), C(2)−C(3) = 1.488(5), C(3)−C(4) = 1.262(6); O(1)−C(1)−Fe(2) = 119.7(2), C(1)−O(1)−C(2) = 117.2(3), O(1)−C(2)−C(3) = 108.8(3), C(4)−C(3)−C(2) = 125.4(5).

available, but coordination to iron of the dangling double bond is nevertheless clear from the spectroscopic data (Tables 1−3). In particular, the presence of only one CO ligand, indicating substitution at iron, is evident in both IR and $^{13}C\{^1H\}$ NMR spectra. Moreover, the three different ligands on iron confer molecular asymmetry, and confirmation of this is provided by the $^{11}B\{^1H\}$ NMR spectrum, which displays a 1:1:1:1:2:1 set of resonances. Other NMR data are likewise consistent with the proposed structure.

It was thought that the C═C bond η-coordinated to the metal center in **9** would be quite readily displaced by addition of strong donor ligands. Thus, treatment with CNXyl (Xyl = $C_6H_3Me_2$-2,6) was expected to afford a species with an {Fe(CO)(CNXyl)(PEt_3)} center and a dangling −O−allyl function. However, addition of an excess of the isocyanide to a CH_2Cl_2 solution of **9** did not result in any observable reaction, as judged by infrared analysis of the mixture. Very surprisingly, though, upon addition of PEt_3 to this mixture, both the allyl group and the remaining CO ligand were replaced by CNXyl groups to afford the compound [2,2-$(CNXyl)_2$-2-PEt_3-1-$OCH_2CH{=}CH_2$-*closo*-2,1,10-$FeC_2B_7H_8$] (**10**), data for which are summarized in Tables 1−3. A single-crystal X-ray diffraction experiment upon this compound revealed the structure shown in Figure 1. This study confirmed the presence of one PEt_3 and two CNXyl substituents bonded to the iron center and a pendant allyl group attached via an oxygen atom to the cage carbon atom adjacent to the iron center. Geometric parameters are within normal ranges and merit little further comment. The NMR spectroscopic data for compound **10** (Tables 2 and 3) are in complete agreement with the solid-state picture.

At first sight, it is perhaps somewhat surprising that the addition of CNXyl to **9**, giving **10**, required an apparent "activation" by addition of PEt_3. Clearly the olefinic group in **9** is more strongly bonded to iron than initially was thought. The

Scheme 1. Proposed Mechanism for the Formation of Compound 10

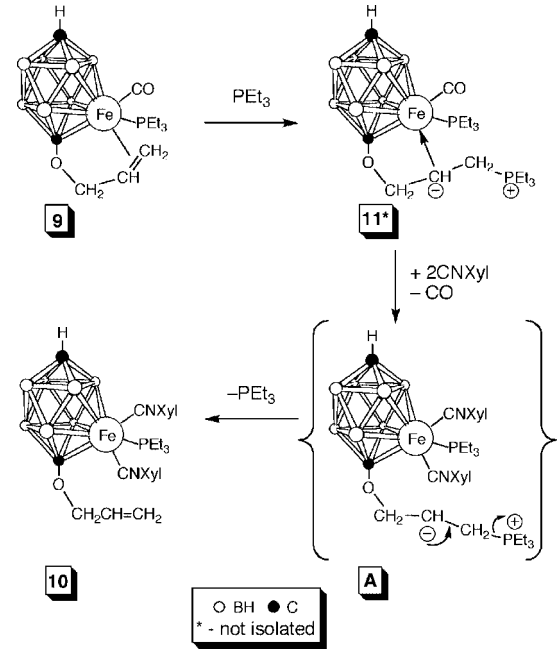

role of the phosphine is believed to be that proposed in Scheme 1. Initial attack of PEt_3 upon **9** results not in a lifting off of the double bond but instead in formation of an ylide compound (**11**) by addition of the phosphine to the terminal iron bound $=CH_2$ unit. There are several precedents for such reactions in metallacarborane chemistry, more usually with *B*,*M*-σ:η^2-vinylic groups.[21] Attack of CNXyl upon the molecule **11** can then result in displacement of the organic ylide function and a CO molecule to give the intermediate **A**, from which PEt_3 loss forms the observed product **10**. In the light of this proposed mechanism, it was of interest to see whether compound **11** itself could be isolated (or at least detected) by treatment of **9** with PEt_3 alone. However, no such evidence could be obtained in preliminary studies, and so the above mechanism must remain somewhat tentative.

Reactions of the C_{cage}−O−Alkynyl Derivatives 7 and 8. In parallel with the above studies on the cage−O−allyl species **6**, a number of experiments were also performed to examine the reactivity of the pendant organic group in the cage−O−propargyl derivative **7**. Thus, for example, it has long been known that carbon−carbon triple bonds can react with $[Co_2(CO)_8]$ to form a $\{C_2Co_2\}$ "tetrahedron";[22] it was hoped that from compound **7** a species could be obtained in which an $\{FeC_2B_7\}$ cluster and a $\{C_2Co_2\}$ tetrahedron are linked via a $-OCH_2-$ bridge. If successful, such a reaction would also verify that the dangling propargyl group retains its acetylenic character despite attachment to the cluster. This proved to be the case, with treatment of **7** with $[Co_2(CO)_8]$ in petroleum ether giving the compound [2,2-$(CO)_2$-2-PEt_3-1-{OCH_2-(μ-η^2:η^2-C≡CH)$Co_2(CO)_6$}-*closo*-2,1,10-$FeC_2B_7H_8$] (**12**) (see Scheme 2) in excellent

(21) Anderson, S.; Mullica, D. F.; Sappenfield, E. L.; Stone, F. G. A. *Organometallics* **1996**, *15*, 1676. Du, S.; Ellis, D. D.; Jelliss, P. A.; Kautz, J. A.; Malget, J. A.; Stone, F. G. A. *Organometallics* **2000**, *19*, 1983.

(22) Dickson, R. S.; Fraser, P. J. *Adv. Organomet. Chem.* **1974**, *12*, 323. Kemmitt, R. D. W.; Russell, D. R. In *Comprehensive Organometallic Chemistry*; Wilkinson, G., Abel, E. W., Stone, F. G. A., Eds.; Pergamon Press: Oxford, U.K., 1982; Vol. 5, Section 34. (c) Sweany, R. L. In *Comprehensive Organometallic Chemistry II*; Abel, E. W., Stone, F. G. A., Wilkinson, G., Eds.; Pergamon Press: Oxford, U.K., 1995; Vol. 8, Chapter 1.

Scheme 2. Reactions of Compounds 7 and 8

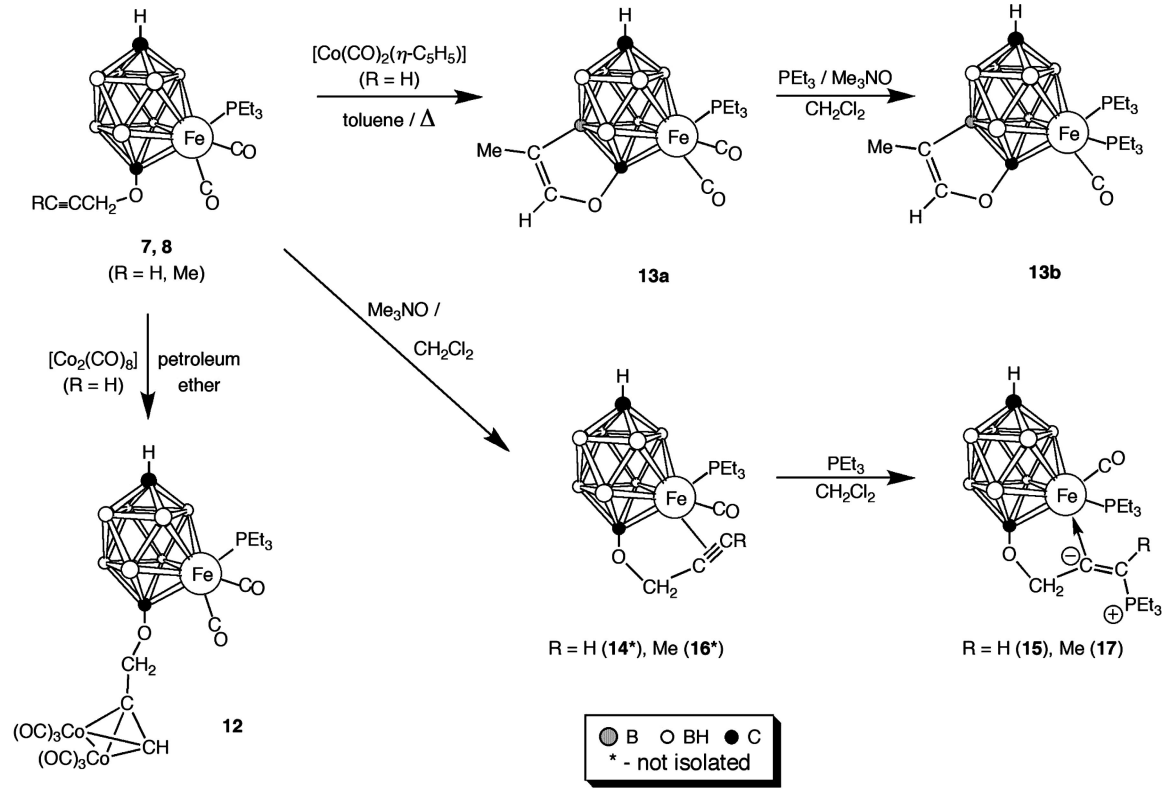

yield. Definitive confirmation that the triple bond in **12** was bonded to the two cobalt centers was provided by an X-ray diffraction experiment, the result of which is shown in Figure 2. The acetylene moiety is bonded in the typical μ-η^2:η^2 mode, and distances within the $\{C_2Co_2\}$ tetrahedron are within normal ranges,[23] with C(12)−C(13) = 1.325(4) Å and Co(1)−Co(2) = 2.4715(4) Å. Spectroscopic data characterizing compound **12** (Tables 1−3) again are consistent with the observed structure, with parameters attributed to the $\{C_2Co_2\}$ tetrahedron also being similar to those reported previously.[24]

In contrast with the reaction between acetylenes and $[Co_2(CO)_8]$ discussed above, the reagent $[Co(CO)_2(\eta\text{-}C_5H_5)]$ is also known to react with C≡C triple bonds, the process typically resulting in acetylene oligomerization processes that include cyclotrimerization or cyclopentadienone formation.[22] It was clearly of interest, therefore, to examine for similar reactivity in the case of compound **7**. Thus, thermolysis of **7** with $[Co(CO)_2(\eta\text{-}C_5H_5)]$ (2 equiv) in refluxing toluene afforded a single ferracarborane product, namely [2,2-$(CO)_2$-2-PEt_3-1,4-μ-{OC(H)=C(Me)-*B*}-*closo*-2,1,10-$FeC_2B_7H_7$] (**13a**; see Scheme 2). The exact nature of this species was not at first clear, and single crystals suitable for a structural study were not readily available. However, treatment of **13a** in CH_2Cl_2 with $PEt_3$and Me_3NO resulted in CO substitution and formation of [2-CO-2,2-$(PEt_3)_2$-1,4-μ-{OC(H)=C(Me)-*B*}-*closo*-2,1,10-$FeC_2B_7H_7$] (**13b**; see Scheme 2), for which an X-ray diffraction analysis was performed, and hence compounds **13** could be identified.

Although compound **13a** is not an acetylene oligomerization product, it was nevertheless of great interest, its structure being deduced from that of compound **13b** shown in Figure 3. (Ultimately, crystals of **13a** were also obtained, and its structure confirmed by X-ray diffraction. The results of that experiment are included as Supporting Information.) Molecules of **13b** consist of the same {*closo*-2,1,10-FeC_2B_7} framework as the parent, but the metal center, of course, now bears two PEt_3 ligands and only a single CO group. In addition, considerable rearrangement of the erstwhile propargyl moiety is evident. Thus, the formerly pendant {$OCH_2C{\equiv}CH$} unit now forms a five-membered COC(H)=C(Me)B ring that involves a cage carbon vertex and its directly bonded oxygen plus an adjacent boron vertex (B(4)), with the terminal B−H hydride from that boron now bonded to the exoskeletal ring. Distances within the external part of the ring confirm that a double bond is localized between C(2) and C(3).

A simple mechanism for the formation of compound **13a** is shown in Scheme 3. It is reasonably supposed that the first step would be coordination of a $\{Co(CO)(\eta\text{-}C_5H_5)\}$ fragment (formed by CO elimination from the cobalt reagent)[22] to the dangling acetylenic moiety of the propargyl group, forming the species **B**. From there, a thermally induced internal rearrangement of the coordinated acetylene group gives the intermediate **C**, from which insertion of this acetylene into a cluster B−H bond would give the observed product **13a**. Other, more elaborate mechanisms are also possible—including ones that involve *two* cobalt centers—although many intermediates can be excluded, as they do not lead to the COC(H)=C(Me)B ring seen in the product.

Spectroscopic data for compounds **13** (Tables 1−3) are entirely consistent with the solid-state structure of **13b**. Thus, for example, the $^{11}B\{^1H\}$ NMR spectra indicate, as expected, a mirror symmetric cage with four resonances in the ratio 1:2:2:2, of which the highest frequency signal in each spectrum—that of unit integral—remains a singlet upon retention of proton

(23) Allen, F. H. *Acta Crystallogr.* **2002**, *B58*, 388. Bruno, I.; Cole, J. C.; Edgington, P. R.; Kessler, M.; Macrae, C. F.; McCabe, P.; Pearson, J.; Taylor, R. *Acta Crystallogr.* **2002**, *B58*, 389.

(24) Aime, S.; Milone, L.; Rossetti, R.; Stanghellini, P. L. *Inorg. Chim. Acta* **1977**, *22*, 135.

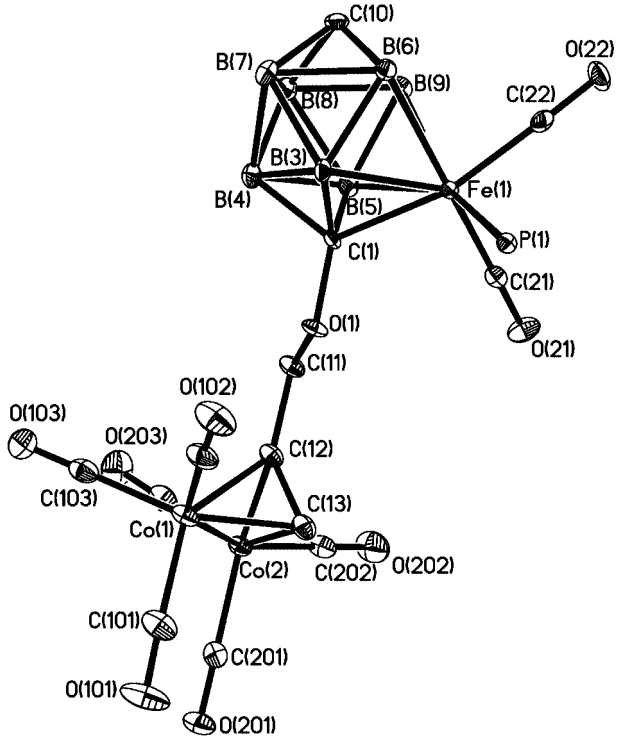

Figure 2. Structure of compound **12** showing the crystallographic labeling scheme. Selected distances (Å) and angles (deg): Fe(1)−C(1) = 1.968(2), Fe(1)−P(1) = 2.2412(6), Fe(1)−C(21) = 1.773(2), Fe(1)−C(22) = 1.773(3), C(1)−O(1) = 1.401(3), O(1)−C(11) = 1.439(2), C(11)−C(12) = 1.483(3), C(12)−C(13) = 1.325(4), Co(1)−Co(2) = 2.4715(4), C(12)−Co(1) = 1.960(2), C(12)−Co(2) = 1.950(2), C(13)−Co(1) = 1.946(3), C(13)−Co(2) = 1.958(2); O(1)−C(1)−Fe(1) = 122.86(15), C(1)−O(1)−C(11) = 115.03(17), O(1)−C(11)−C(12) = 106.83(18), C(13)−C(12)−C(11) = 141.9(2), C(11)−C(12)−Co(1) = 133.44(17), C(11)−C(12)−Co(2) = 135.03(17), Co(1)−C(12)−Co(2) = 78.39(9), Co(1)−C(13)−Co(2) = 78.56(9).

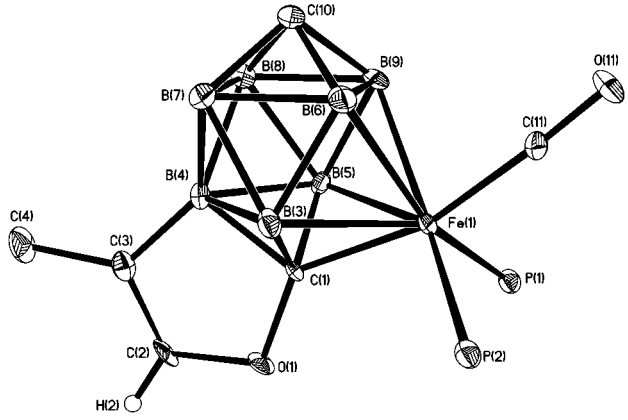

Figure 3. Structure of compound **13b** showing the crystallographic labeling scheme. Selected distances (Å) and angles (deg): Fe(1)−C(1) = 1.941(5), Fe(1)−P(1) = 2.2600(16), Fe(1)−P(2) = 2.2765(17), Fe(1)−C(11) = 1.753(5), C(1)−O(1) = 1.426(6), O(1)−C(2) = 1.380(6), C(2)−C(3) = 1.340(8), C(3)−B(4) = 1.544(8), C(3)−C(4) = 1.510(8); O(1)−C(1)−Fe(1) = 132.6(4), O(1)−C(1)−B(4) = 106.0(4), C(2)−O(1)−C(1) = 108.3(4), C(3)−C(2)−O(1) = 117.4(5), C(2)−C(3)−C(4) = 124.0(5), C(2)−C(3)−B(4) = 106.9(5), C(4)−C(3)−B(4) = 129.1(5), C(3)−B(4)−C(1) = 101.3(4).

coupling and therefore can be assigned to B(4), which bears the exopolyhedral organic substituent. The C and H atoms of the $\overline{\text{COC(H)=C(Me)B}}$ ring appear in diagnostic positions: in the ^{1}H NMR spectrum, the =CH proton is seen at δ 8.00 (**13a**) and 8.02 (**13b**), while the =CMe protons resonate at δ 1.78 (**13a**) and 1.81 (**13b**). In the $^{13}C\{^1H\}$ NMR spectrum, the two olefinic carbons give rise to peaks at δ 169.3 (**13a**) and 167.4 (**13b**) (=CH), and at δ 129.5 (**13a**) and 127.9 (**13b**) (=*C*(Me)), the signals for the latter carbons being significantly broadened by the adjacent quadrupolar boron atom.

In addition to the above formation of a five-membered ring involving a cluster boron atom, it was clearly also of interest to establish whether the dangling triple bond in compound **7** could form an intramolecular bond to the iron center, similar to the arrangement in compound **9**. Thus, treatment of CH_2Cl_2 solutions of **7** with Me_3NO was expected to afford [2-CO-2-PEt_3-1,2-σ:η^2-$OCH_2C{\equiv}CH$-*closo*-2,1,10-$FeC_2B_7H_8$] (**14**; see Scheme 2). However, no reaction was evident, either as a color change or by spectroscopic analysis of the reaction mixture. Instead, treatment of the reaction mixture with PEt_3 afforded a deep red compound that was isolated and identified (see below) as [2-CO-2-PEt_3-1,2-μ-{OCH_2C{=C(H)PEt_3}}-*closo*-2,1,10-$FeC_2B_7H_8$] (**15**; Scheme 2). The observation of the ylide moiety in **15** does support the intermediacy of **14**: attack of PEt_3 upon the terminal carbon atom of the acetylene group would involve activation through metal coordination.[21] (Notably, also, compounds **13b** and **15** are structural isomers!) In parallel with this reaction, similar treatment of complex **8** with PEt_3 and Me_3NO also affords the zwitterionic species **17**, presumed likewise to form via the π-bound acetylene complex **16** (Scheme 2).

Initial confirmation of the constitution of compounds **15** and **17** was via X-ray diffraction studies; the results for the latter complex are deposited as Supporting Information. The structure of one of the crystallographically independent molecules of compound **15** is presented in Figure 4. Therein can be seen the iron-bound ylide group $\overline{\text{FeCOCH}_2\text{C}}${=C(H)$PEt_3$}, the Fe−C σ bond of which forms part of a five-membered ring. Distances within this moiety are all consistent with the structure shown in Scheme 2, and in particular with a C=C double bond being located between C(3) and C(4) and a direct σ bond from C(3) to the Fe center. Spectroscopic parameters for compounds **15** and **17** likewise also concur with the solid-state structure of **15**.

Conclusion

The unusual synthesis of the 10-vertex *dic*arbon carbametallaborane cluster in **3**, starting from the *mono*carbon substrate [*closo*-1-CB_7H_8]$^-$ plus [$Fe_2(CO)_9$], has been demonstrated. Although the dicarbametallaboranes generally constitute the largest class of metal−(hetero)borane cluster species,[1] compounds with fewer than 12 vertices remain relatively rare, and the present work contributes several novel members to the latter category. In **3** the second cluster carbon vertex evidently comes from one of the iron-bound carbonyl ligands of the starting substrate, and thus **3** and its derivatives all contain an oxygen functionality directly bonded to that cage carbon atom. The attachment of substituents to boron clusters is an area where much current effort is focused. Of particular interest, therefore, has been the introduction of a variety of organic functional groups, bonded to the cluster surface via the C_{cage}−O moiety, and this in turn has led to a variety of unusual species such as those containing intramolecular 5-membered rings, exemplified by compounds **13** and **15**. The present compounds, of course, represent only very simple derivatives of **3**, and we are working to expand upon these results in several directions.

Scheme 3. Proposed Mechanism for the Formation of Compound 13a

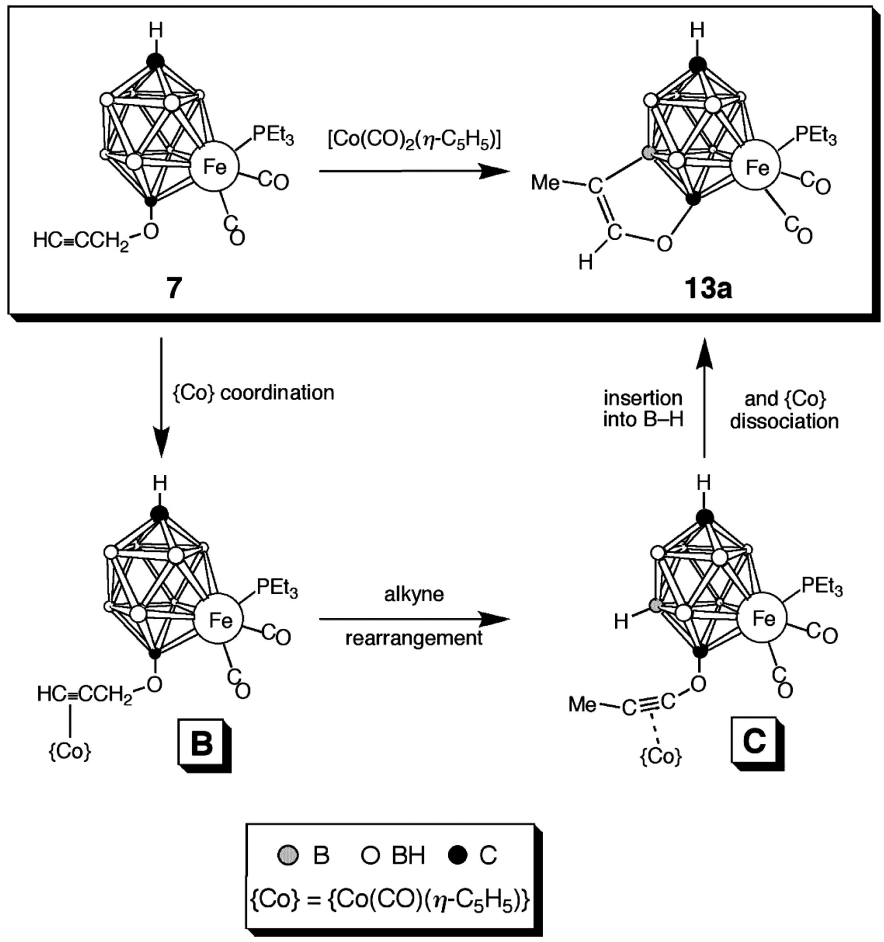

Experimental Section

General Considerations. All reactions were carried out under an atmosphere of dry nitrogen using standard Schlenk line techniques. Solvents were stored over and distilled from appropriate drying agents under nitrogen prior to use. Petroleum ether refers to that fraction of boiling point 40–60 °C. Chromatography columns (ca. 20 cm in length and ca. 2 cm in diameter) were packed with silica gel (Acros, 60–200 mesh). NMR spectra were recorded at the following frequencies (MHz): ^{1}H, 360.13; ^{13}C, 90.56; ^{11}B, 115.5; ^{31}P, 145.78. Elemental analyses were performed by Atlantic Microlab, Inc., Norcross, GA, upon crystalline or microcrystalline samples that had been dried overnight in vacuo. On occasion residual solvent remained after drying, its presence and approximate proportion confirmed by integrated ^{1}H NMR spectroscopy, and this was factored into the calculated microanalysis data. Sodium hydride, supplied as a 60% suspension in mineral oil (Aldrich), was washed with petroleum ether (2 × 10 mL) and dried in vacuo immediately prior to use, and HC≡CCH$_2$Br was used as an 80% solution in toluene. The carborane salt [NBu$^{n}_{4}$][*closo*-1-CB$_7$H$_8$] was synthesized according to the literature method;[5e] all other materials were used as supplied.

Synthesis of [2,2-(CO)$_2$-2-L-1-OH-*closo*-2,1,10-FeC$_2$B$_7$H$_8$] (L = CO (3), PEt$_3$ (4)). (i) [NBu$^{n}_{4}$][*closo*-1-CB$_7$H$_8$] (0.20 g, ca. 0.6 mmol) was dissolved in THF (15 mL), solid [Fe$_2$(CO)$_9$] (0.45 g, 1.2 mmol) was added, and the mixture was heated under reflux for 18 h. After the mixture was cooled to ambient temperature, volatiles were removed under reduced pressure, the residue was dissolved in neat CH$_2$Cl$_2$ (5 mL), and this solution was transferred to the top of a short (10 cm) chromatography column. Elution with CH$_2$Cl$_2$ gave a deep red fraction that was collected, concentrated to 15 mL by evaporation, and treated with CF$_3$SO$_3$H (0.25 mL, ca. 4 mmol), added dropwise. After the mixture was stirred for 15 min, solvent was removed under reduced pressure and the resulting green residue was dissolved in CH$_2$Cl$_2$ (2 mL) and subjected to column chromatography as above, giving a fast-moving, deep green fraction (identified as [Fe$_3$(CO)$_{12}$]) followed by a yellow fraction. The latter was collected and solvent removed in vacuo to afford yellow microcrystals of **3** (0.08 g, 52%).

(ii) Similarly, a THF (15 mL) solution containing [NBu$^{n}_{4}$][*closo*-1-CB$_7$H$_8$] (0.20 g, ca. 0.6 mmol) and [Fe$_2$(CO)$_9$] (0.45 g, 1.2 mmol) was heated to reflux for 18 h, and cooled, and then the volatiles were removed under reduced pressure. The residue was dissolved in neat CH$_2$Cl$_2$ (15 mL), PEt$_3$ (0.9 mL, 5 mmol) and Me$_3$NO (0.10 g, 1.33 mmol) were added, and the mixture was stirred at room temperature for 2 h. Removal of solvent in vacuo yielded a brown residue, which was dissolved in CH$_2$Cl$_2$/petroleum ether (3:2, 2 mL) and applied to a chromatography column. Eluting with the same mixture gave a yellow fraction that was collected and evaporated in vacuo to give yellow microcrystals of **4** (0.13 g, 61%).

Synthesis of [2,2-(CO)$_2$-2-PEt$_3$-1-OR-*closo*-2,1,10-FeC$_2$B$_7$H$_8$] (R = Me (5), CH$_2$CH=CH$_2$ (6), CH$_2$C≡CH (7), CH$_2$C≡CMe (8)). (i) Compound **4** (ca. 0.18 g, 0.5 mmol) was dissolved in THF (20 mL), the solution was added to NaH (0.2 g, 5 mmol), and the mixture was stirred at ambient temperature for 15 min. Excess NaH was removed by filtration, MeI (ca. 0.07 mL, 1 mmol) was added to the filtrate, and the resultant mixture was stirred at ambient temperature for 18 h. Volatiles were removed in vacuo, and the residue was dissolved in CH$_2$Cl$_2$/petroleum ether (1:1, 2 mL) and transferred to the top of a chromatography column. Elution with the same mixture gave a yellow fraction, from which removal of solvent in vacuo yielded yellow microcrystals of **5** (0.15 g, 84%).

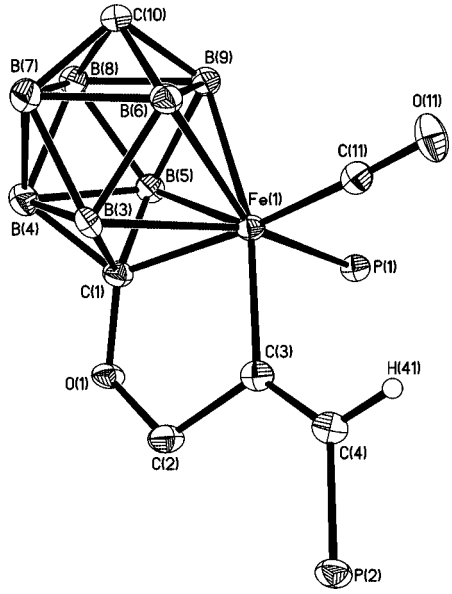

Figure 4. Structure of one of the crystallographically independent molecules of compound **15** showing the crystallographic labeling scheme. Selected distances (Å) and angles (deg): Fe(1)−C(1) = 1.927(3), Fe(1)−P(1) = 2.2118(9), Fe(1)−C(11) = 1.736(3), Fe(1)−C(3) = 1.961(3), C(1)−O(1) = 1.409(3), O(1)−C(2) = 1.428(3), C(2)−C(3) = 1.534(4), C(3)−C(4) = 1.353(4), C(4)−P(2) = 1.772(3); C(11)−Fe(1)−C(3) = 97.51(13), C(3)−Fe(1)−P(1) = 87.62(8), C(1)−Fe(1)−C(3) = 79.93(12), O(1)−C(1)−Fe(1) = 117.40(18), C(1)−O(1)−C(2) = 108.6(2), O(1)−C(2)−C(3) = 110.9(2), C(4)−C(3)−C(2) = 118.1(3), C(4)−C(3)−Fe(1) = 128.3(2), C(2)−C(3)−Fe(1) = 113.35(18), C(3)−C(4)−P(2) = 128.5(3).

Further elution with CH_2Cl_2/petroleum ether (4:1) allowed recovery of unreacted **4** (ca. 0.02 g, 10%).

(ii) Similarly, compound **4** (ca. 0.18 g, 0.5 mmol), NaH (60%) (0.2 g, 5 mmol), and $CH_2{=}CHCH_2Br$ (ca. 0.09 mL, 1 mmol) yielded yellow microcrystals of **6** (0.15 g, 77%), along with unreacted **4** (ca. 0.025 g, 14%).

(iii) By an analogous procedure, compound **4** (ca. 0.18 g, 0.5 mmol), NaH (0.2 g, 5 mmol), and $HC{\equiv}CCH_2Br$ (ca. 0.1 mL, 1 mmol) gave yellow microcrystals of **7** (0.12 g, 65%) plus unreacted **4** (ca. 0.037 g, 21%).

(iv) Similarly, compound **4** (ca. 0.18 g, 0.5 mmol), NaH (0.2 g, 5 mmol), and $MeC{\equiv}CCH_2Br$ (ca. 0.09 mL, 1 mmol) afforded yellow microcrystals of **8** (0.12 g, 65%) followed by unreacted **4** (ca. 0.037 g, 21%).

Synthesis of [2-CO-2-PEt$_3$-1,2-σ:η^2-OCH$_2$CH=CH$_2$-*closo*-2,1,10-FeC$_2$B$_7$H$_8$] (9). Compound **6** (0.18 g, 0.5 mmol) was dissolved in CH_2Cl_2 (20 mL), Me_3NO (0.08 g, 1 mmol) was added, and the mixture was stirred at room temperature for 48 h. After evaporation in vacuo the residue was dissolved in CH_2Cl_2/petroleum ether (3:2, 2 mL) and transferred to the top of a chromatography column. Elution with the same solvent mixture afforded a small quantity of unreacted **6** (0.01 g, 5%). Thereafter, elution with CH_2Cl_2/petroleum ether (4:1) gave a yellow fraction, removal of solvent from which in vacuo yielded yellow microcrystals of **9** (ca. 0.17 g, 92%).

Synthesis of [2,2-(CNXyl)$_2$-2-PEt$_3$-1-OCH$_2$CH=CH$_2$-*closo*-2,1,10-FeC$_2$B$_7$H$_8$] (10). Compound **9** (0.18 g, 0.5 mmol) was dissolved in CH_2Cl_2 (20 mL), CNXyl (0.13 g, 1 mmol) and PEt_3 (0.25 mL, 1.7 mmol) were added, and the mixture was stirred at ambient temperature for 18 h. Solvent was evaporated in vacuo, and the residue was dissolved in CH_2Cl_2/petroleum ether (3:2, 2 mL) and transferred to the top of a chromatography column. Elution with the same mixture gave an orange fraction that was collected and evaporated in vacuo to obtain orange microcrystals of **10** (0.25 g, 84%). Thereafter, elution with CH_2Cl_2/petroleum ether gave a yellow fraction that contained a small quantity of unreacted **9** (ca. 0.02 g, 8%).

Synthesis of [2,2-(CO)$_2$-2-PEt$_3$-1-{OCH$_2$-(μ-η^2:η^2-C≡CH)Co$_2$(CO)$_6$}-*closo*-2,1,10-FeC$_2$B$_7$H$_8$] (12). To a solution of compound **7** (ca. 0.20 g, 0.5 mmol) in *n*-hexane (20 mL) was added [$Co_2(CO)_8$] (0.17 g, 0.51 mmol), and the resulting mixture was stirred at ambient temperature for 18 h. Volatile components were removed in vacuo, and the residue was taken up in petroleum ether (2 mL) and applied to a chromatography column. Elution with petroleum ether removed unreacted [$Co_2(CO)_8$], and then elution with CH_2Cl_2/petroleum ether (1:4) gave an orange fraction that was evaporated in vacuo to yield yellow microcrystals of **12** (0.31 g, 91%).

Synthesis of [2-CO-2-PEt$_3$-2-L-1,4-μ-{OC(H)=C(Me)-*B*}-*closo*-2,1,10-FeC$_2$B$_7$H$_7$] (L = CO (13a), PEt$_3$ (13b)). (i) Compound **7** (ca. 0.19 g, 0.5 mmol) was dissolved in toluene (20 mL), [$Co(CO)_2(\eta$-$C_5H_5)$] (0.17 g, 1 mmol) was added, and the solution was vigorously heated at reflux temperature for 18 h. After cooling and removal of volatiles in vacuo, the residue was extracted into petroleum ether (2 mL) and the solution transferred to a chromatography column. Elution with the same solvent removed residual cobalt species, and then elution with CH_2Cl_2/petroleum ether (1:4) gave a yellow fraction. Removal of solvents from the latter yielded yellow microcrystals of **13a** (0.10 g, 53%).

(ii) Compound **13a** (0.10 g, 0.25 mmol) was dissolved in CH_2Cl_2 (10 mL), and PEt_3 (0.14 mL, 1.0 mmol) and Me_3NO (ca. 0.8 g, 1 mmol) were added. The solution was stirred at room temperature and evaporated to dryness, and the residue was taken up in CH_2Cl_2/petroleum ether (1:4, 1 mL) and subjected to column chromatography. Elution with the same solvent mixture gave a yellow fraction, from which were obtained yellow microcrystals of **13b** (0.08 g, 62%).

Synthesis of [2-CO-2-PEt$_3$-1,2-μ-{OCH$_2$C{=C(R)PEt$_3$}}-*closo*-2,1,10-FeC$_2$B$_7$H$_8$] (R = H (15), Me (17)). (i) To a solution of **7** (ca. 0.19 g, 0.5 mmol) in CH_2Cl_2 (20 mL) were added PEt_3 (0.5 mL, 3.4 mmol) and Me_3NO (0.1 g, 1.3 mmol), and the resulting mixture was stirred for 24 h at room temperature. Volatiles were removed in vacuo, the residue was dissolved in CH_2Cl_2 (2 mL), and petroleum ether (8 mL) was added to precipitate a red solid. The latter was collected by filtration, washed with petroleum ether (3 × 10 mL), and dried in vacuo, giving red microcrystals of **15** (0.15 g, 62%).

(ii) Similarly, reaction of **8** (ca. 0.20 g, 0.5 mmol), PEt_3 (0.5 mL, 3.4 mmol), and Me_3NO (0.1 g, 1.3 mmol) gave red microcrystals of **17** (0.13 g, 54%).

X-Ray Crystallographic Structure Determinations. Experimental data for **10**, **12**, **13b**, and **15** are presented in Table 4. Details of the structure determinations for **13a** and **17** have been deposited as Supporting Information. X-ray intensity data were collected at 110(2) K on a Bruker-Nonius X8 APEX CCD area-detector diffractometer using Mo Kα X-radiation. Several sets of narrow data "frames" were collected at different values of θ, for various initial values of φ and ω, using 0.5° increments of φ or ω. The data frames were integrated using SAINT;[25] the substantial redundancy in data allowed an empirical absorption correction (SADABS)[25] to be applied, based on multiple measurements of equivalent reflections.

All structures were solved using conventional direct methods[25,26] and refined by full-matrix least squares on all F^2 data using SHELXTL version 6.12,[26] with anisotropic thermal parameters assigned to all non-H atoms. The locations of the cage-carbon atoms were verified by examination of the appropriate internuclear distances and the magnitudes of their isotropic thermal displacement parameters. Cluster BH and CH hydrogens, with the exception of those in compound **13b**, were allowed positional refinement; all other H atoms were set riding in calculated positions. All hydrogen atoms had fixed isotropic thermal

(25) *APEX 2, version 1.0*; Bruker AXS, Madison, WI, 2003–2004.
(26) *SHELXTL, version 6.12*; Bruker AXS, Madison, WI, 2001.

Table 4. Crystallographic Data for Compounds 10, 12, 13b, and 15

	10·0.5C_5H_{12}	**12**	**13b**	**15**·0.5CH_2Cl_2
formula	$C_{31.5}H_{52}B_7FeN_2OP$	$C_{19}H_{26}B_7Co_2FeO_9P$	$C_{18}H_{41}B_7FeO_2P_2$	$C_{18.5}H_{42}B_7ClFeO_2P_2$
fw	637.24	678.75	482.97	525.43
space group	$P2_1/n$	$P\bar{1}$	$P\bar{1}$	$P\bar{1}$
a, Å	13.040(3)	7.5362(3)	8.7786(6)	12.2721(15)
b, Å	15.018(3)	8.3695(4)	9.8596(7)	14.7948(18)
c, Å	18.379(4)	23.0178(10)	15.0003(11)	17.112(2)
α, deg	90	84.158(2)	85.101(4)	106.637(6)
β, deg	90.564(15)	83.378(3)	79.204(3)	107.820(6)
γ, deg	90	83.582(2)	82.038(3)	98.800(6)
V, Å^3	3599.1(14)	1427.28(11)	1260.69(15)	2733.7(6)
Z	4	2	2	4
ρ_{calcd}, g cm^{-3}	1.176	1.579	1.272	2733.7(6)
μ(Mo Kα), mm^{-1}	0.490	1.751	0.738	0.781
no. of rflns measd	43 480	21 657	15 898	41 181
no. of indep rflns	8387	6868	4990	12 351
R_{int}	0.1194	0.0469	0.0521	0.0716
wR2, R1[a] (all data)	0.1339, 0.1348	0.0747, 0.0587	0.1900, 0.0930	0.1023, 0.0870
wR2, R1 (obsd[b] data)	0.1065, 0.0574	0.0674, 0.0373	0.1832, 0.0764	0.0863, 0.0482

[a] $wR2 = [\sum\{w(F_o^2 - F_c^2)^2\}/\sum w(F_o^2)^2]^{1/2}$; $R1 = \sum||F_o| - |F_c||/\sum|F_o|$. [b] $F_o > 4\sigma(F_o)$.

parameters defined as $U_{iso}(H) = 1.2 \times U_{iso}$(parent), or $U_{iso}(H) = 1.5 \times U_{iso}$(parent) for methyl groups.

Molecules of **10** cocrystallized each with a half-molecule of *n*-pentane in the asymmetric fraction of the unit cell. The γ-CH_2 unit of the solvate lay at an inversion center, while the β-CH_2 unit was disordered over two positions, these being modeled as each being 50% occupied. Two independent molecules of compound **15** cocrystallized with one molecule of CH_2Cl_2 in the asymmetric unit. This solvate was located in general space and refined without difficulty.

Acknowledgment. We thank the Robert A. Welch Foundation and Baylor University for support. The Bruker-Nonius X8 APEX diffractometer was purchased with funds received from the National Science Foundation Major Instrumentation Program (Grant No. CHE-0321214).

Supporting Information Available: Full details of the crystal structure analyses in CIF format, including data for compounds **13a** and **17**. This material is available free of charge via the Internet at http://pubs.acs.org.

OM700865S